Inorganic Chemistry

ARTICLE

pubs.acs.org/IC

Cyclam-methylbenzimidazole: a Selective OFF-ON Fluorescent Sensor for Zinc

Abir El Majzoub,[†] Cyril Cadiou,[†] Isabelle Déchamps-Olivier,[†] Bernard Tinant,[‡] and Françoise Chuburu*[,†]

[†]Groupe Chimie de Coordination, Institut de Chimie Moléculaire de Reims, Université Reims-Champagne-Ardenne, UMR 6229, C2POM, Bât. 18, BP 1039, 51687 Reims Cedex 2, France

[‡]MOST, Institute of Condensed Matter and Nanosciences (IMCN), Université catholique de Louvain, Place Louis Pasteur, B-1348 Louvain-la-Neuve, Belgium

Supporting Information

ABSTRACT: The coordination properties and the photophysical response of a new cyclam fluorescent probe for Zn(II), [**L1**H: 1-(benzimidazol-2-ylmethyl]-1,4, 8,11-tetraazacyclotetradecane] toward Cu(II), Zn(II), and Cd(II) are reported. The stability constants of the corresponding complexes were determined by means of potentiometric measurements in aqueous solution. The fluorescence of **L1**H was quenched by the presence of Cu(II), and **L1**H behaves as an OFF-ON sensor for Zn(II) even in the presence of a wide range of biological divalent cations. Furthermore, on addition of successive amounts of Zn(II), the fluorescence emission of **L1**H increases linearly by a factor of 12. This can be correlated to the efficient Zn(II) binding of **L1**H and to the participation of all the amine functions in the metal coordination which prevents the photoinduced electron transfer (PET) effect and promotes a good chelation-enhanced fluorescence (CHEF) effect; this confers to the cyclam probe better sensing properties than the cyclen ionophore.

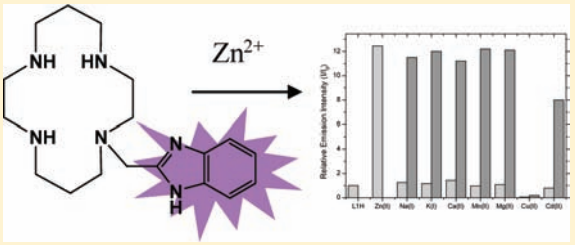

INTRODUCTION

The detection of trace elements implicated in biological events as well as in environmental issues is still a great challenge and requires effective sensors.[1] Among these elements, zinc is probably one of the most important with iron, and its physiological importance has been recognized.[2] The most important and best-known role for zinc is as a structural cofactor in metalloproteins. Many zinc proteins possessing one or more zinc motifs have been identified.[3] A catalytic role was also identified for zinc for instance in carbonic anhydrase or carboxypeptidase,[4] and recently the neurological roles of zinc have attracted a lot of attention.[5] Diseases such as Alzheimer's disease, amyotrophic lateral sclerosis, Parkinson's disease, and epilepsy can be ascribed to disorder in zinc metabolism. In this context, the development of fluorescent chemosensors[6] with high selectivity for zinc represents an important challenge for this spectroscopically silent ion. A typical chemosensor contains a receptor (the recognition site) with binding selectivity linked to a signaling unit (the signal source) which converts the recognition event to an optical signal. The most applied fluorescence mechanisms which allow the signal transduction in this context are mainly internal charge transfer (ICT) and photoinduced electron transfer (PET).[7] For PET chemosensors, a fluorophore is usually connected via a spacer to a receptor containing relatively high-energy nonbonding electron pair (such as a nitrogen atom) which can transfer an electron to the excited fluorophore and as a result, quenches the fluorescence. When the electron pair is shared by coordination to a cation, the redox potential of the receptor is raised so that the highest occupied molecular orbital (HOMO) of the receptor becomes lower in energy than that of the fluorophore. Thus, the PET process from the receptor to the fluorophore is inefficient, and the fluorescence is restored (chelation-enhanced fluorescence effect, CHEF).[8]

Currently, there is still a significant interest in the development of more effective probes that are water-soluble and for which the complexation with the metal of interest is stoichiometric (ML complexes). For that, azamacrocycles are well suited toward divalent cations. Among the azamacrocycles, cyclen is probably the most used for this purpose and has demonstrated its ability to be a good ligand in a number of PET-based probes.[9] We recently reported the synthesis of a cyclen-based fluorescent sensor in which the fluorescent unit is constituted of a benzimidazole ring.[10] This fluorophore was chosen first according to the affinity in metalloenzymes of zinc for the imidazole of histidine units and second for its ability to behave as an efficient coordinating motif for "scorpion-like" complexes.

We envisaged that the performance of cyclen-methylbenzimidazole could be improved through the development of cyclam-methylbenzimidazole **L1**H (Scheme 1). We were encouraged to evaluate this new ligand as a chemical sensor for zinc by recent results obtained by Watkinson et al.[11] with "click"-generated cyclam fluorophores. The present paper describes the coordination and optical properties of cyclam-methylbenzimidazole **L1**H,

Received: December 17, 2010
Published: April 05, 2011

Scheme 1

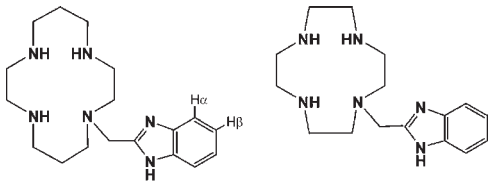

L1H **L2H**

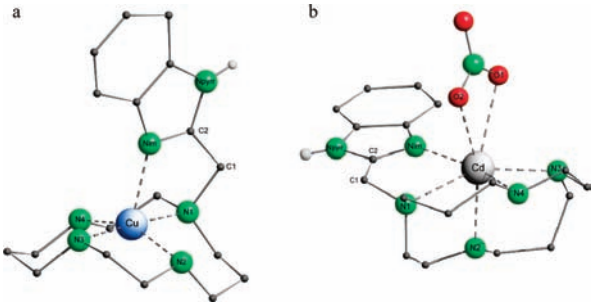

Figure 1. (a) $[Cu(\mathbf{L1}H)]^{2+}$ and (b) $[Cd(\mathbf{L1}H)(NO_3)]^{+}$ crystal structures; hydrogen atoms are omitted for clarity, except the pyrrolic one.

synthesized via the two-step bisaminal methodology,[12] toward Cu(II), Zn(II), and Cd(II). Two important points were particularly assessed (i) the thermodynamical stability of the complexes and (ii) the specific photochemical response to zinc coordination.

RESULTS AND DISCUSSION

Coordination Chemistry of L1H. To investigate the coordination chemistry of **L1**H with Cu(II), Zn(II), and Cd(II) either in the solid state or in solution, complexes of **L1**H were prepared by treatment of their methanolic solution with 1 equiv of the corresponding metal salts. Single crystals suitable for X-ray diffraction were obtained for $[Cu(\mathbf{L1}H)](BF_4)_2$, and $[Cd\mathbf{L1}H(NO_3)](NO_3)$ by slow diffusion of diethyl ether into methanol and acetonitrile solutions of the complexes, respectively. Zinc(II), cadmium(II), and copper(II) complexes were subsequently characterized in solution by means of NMR, UV−vis, and EPR spectroscopies.

The crystal structure of $[Cu(\mathbf{L1}H)]^{2+}$ complex (Figure 1a) shows that the metal ion is pentacoordinated by the four nitrogen atoms of the cyclam unit and the imine nitrogen atom of the substituent (Nim) in the axial fifth position. The Cu(II) center is located 0.27 Å above the mean square plane constituted by the macrocyclic nitrogen atoms. According to Bonisch nomenclature,[13] the complex exhibits a type I (*R*, *S*, *R*, *S*) (++++) configuration where + indicates that the NH group is above the plane of the macrocycle. The bond distances and angles defining the coordination sphere (Table S1, Supporting Information) are those expected for this kind of metal complex.[13b] To check if the metal pentacoordination is maintained in solution, the visible spectra of $[Cu(\mathbf{L1}H)](BF_4)_2$ were recorded in solid state and in solution (Figure S1, Supporting Information). In the solid state the Cu(II) absorption appears as a broad signal around 625 nm while in water, $[Cu\mathbf{L1}H]^{2+}$ shows an absorption maximum at 618 nm (ε = 110 M^{-1} cm^{-1}). The spectra similarity tends to prove that the geometry in the solid state is retained in solution.[14] Furthermore, the

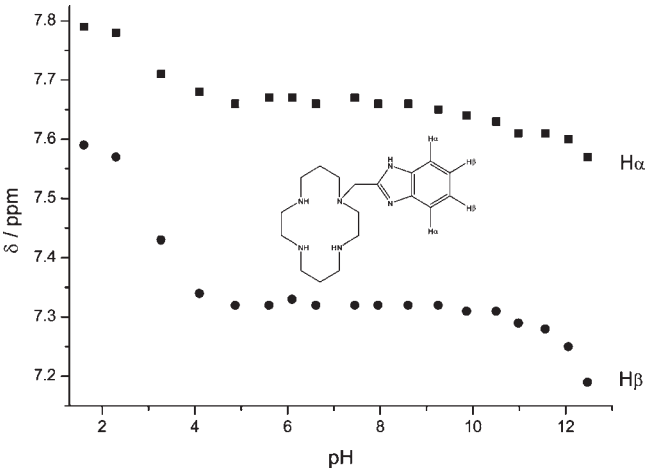

Figure 2. ^{1}H NMR chemical shifts evolution for **L1**H (10^{-2} mol dm^{-3}) in the pH range 2.0−12.0 (T = 298.1 K, D_2O).

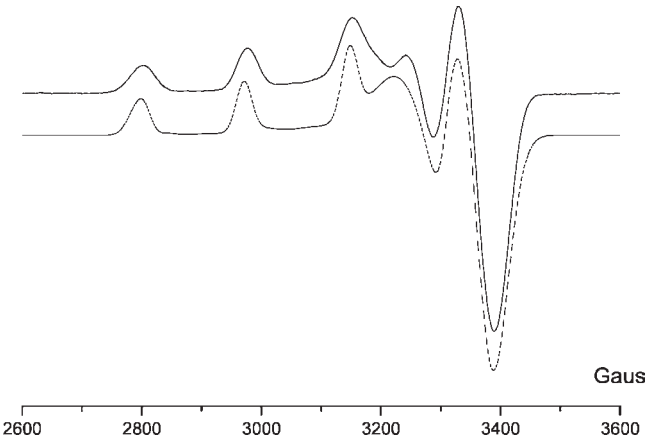

Figure 3. EPR spectrum of $[Cu\mathbf{L1}H]^{2+}$ in frozen water (180 K) (experimental, plain lines; simulated, dotted lines).

electron paramagnetic resonance (EPR) spectrum of $[Cu(\mathbf{L1}H)](BF_4)_2$ in frozen solution (Figure 3) exhibits a strong absorption at about 3200 G, attributable to the allowed transitions $\Delta M_S = 1$. The shape of the spectrum consists of four equidistant absorptions in the parallel region as expected for the coupling of the unpaired copper electron with the copper nucleus (I = 3/2). The EPR parameters $g_{\|} = 2.197 > g_{\perp} = 2.041$ and $G = (g_{\|} - 2)/(g_{\perp} - 2) > 4$ (Table S2, Supporting Information) are typical of axially symmetric d^9 copper(II) complexes in a ground-state doublet, with the unpaired electron in the $d_{x^2-y^2}$ orbital.[15] Furthermore, the $A_{\|}$ value for $[Cu\mathbf{L1}H]^{2+}$ is smaller than the corresponding $A_{\|}$ value for the parent complex[16] $[Cu(1,4,8,11\text{-tetraazacyclotetradecane})]^{2+}$ and very similar to the one determined for $[Cu(1\text{-(pyridin-2-ylmethyl)-}1,4,8,11\text{-tetraazacyclotetradecane})]^{2+}$ in which the pyridine nitrogen atom is coordinated to the copper center.[13a] The visible and EPR data agreed then to indicate that even in solution, the $[Cu\mathbf{L1}H]^{2+}$ geometry is square-pyramidal with a pentacoordinated copper center (Cu(II)-N_5 chromophore).

The crystal structure of $[Cd\mathbf{L1}H(NO_3)]^{+}$ (Figure 2b) shows that the metal ion is heptacoordinated by four macrocyclic nitrogen atoms, one imine nitrogen atom from the pendant arm, and two oxygen atoms from one coordinated nitrate ion. The distances between Cd(II) and nitrogen atoms of the benzimidazole group are

dx.doi.org/10.1021/ic102521g |*Inorg. Chem.* 2011, 50, 4029–4038

similar (Table S1, Supporting Information) and fall within the range reported for Cd−N distances in complexes with ligands containing benzimidazole groups.[17] The geometry around the metal ion can be described as distorted capped octahedral, or distorted octahedral if both coordinated oxygen atoms of the nitrate anion are considered to occupy one coordination position. The average Cd−O bond length (2.540 Å) is in accordance with the distance found in Cd(II) complexes where the nitrate ion is coordinated to the Cd(II) ion in such a bidentate fashion.[18] Finally, in $[Cd\mathbf{L1}H(NO_3)]^+$ the macrocyclic cavity adopts a cis-folded configuration leading to a type V (*R*, *R*, *R*, *R*) (+ − + −) configuration.[13a] This configuration is imposed by the equatorial coordination of the benzimidazole pendant arm and the axial coordination of the nitrate ion.[18a] To have an insight into the $[Cd\mathbf{L1}H]^{2+}$ structure in solution, its ^1H and ^{13}C NMR spectra were recorded (see Experimental Section). It is known that for benzimidazole appended ligands, the aromatic region of the NMR spectrum appears to be a good probe to test the coordination of the benzimidazole to the metal ion.[19] While the ^{13}C NMR spectrum of **L1**H shows only four resonances in the aromatic region, the ^{13}C NMR spectrum of $[Cd\mathbf{L1}H](NO_3)_2$ presents seven resonances in the aromatic carbon area. Then the aromatic region seems to be more clearly resolved for the metal ion complex than for the free ligand. This is due to the presence in the latter of exchange processes involving the NH and N positions of the benzimidazole groups that are prevented by coordination to the metal ion. Then, it can be concluded that in solution, the benzimidazole substituent is still coordinated to the metal ion. Furthermore, in the $[Cd\mathbf{L1}H](NO_3)_2$ ^1H NMR spectrum, the two inner aromatic protons (Hα, Scheme 1) of the benzimidazole are not equivalent (δ = 7.63 and 7.68 ppm) while the two outer aromatic protons (Hβ, Scheme 1) are undifferentiated (δ = 7.38 ppm) (Figure S2, Supporting Information). This has not been observed for **L1**H and could be the result of the coordination of one of the two nitrate ions to Cd(II), leading to three sets of aromatic protons. From this first analysis, it seems that the Cd(II) coordination sphere is preserved in solution. Finally, the ^1H NMR spectrum of $[Cd\mathbf{L1}H]^{2+}$ shows that the ^1H NMR spectrum[20] appeared, particularly for the two protons of the methylene linker, as two doublets of doublets (δ = 3.94 ppm and 4.35 ppm ^2J = 17 Hz and 4.05 ppm and 4.25 ^2J = 17.06 Hz, (Figure S2, Supporting Information). In a previous work, Sadler et al. reported a similar situation for $[Zn_2$-xylyl (bis-cyclam)$]^{4+}$ and demonstrated that it has to be associated to the presence of isomers in solution, distinguishable by the presence of different spin systems for the methylene linker protons particularly.[21] The methylene signals observed for $[Cd\mathbf{L1}H]^{2+}$, as well as the presence of weak peaks in the region of aromatic protons, can then be correlated to the presence of isomers in solution. It should also be noted that for $[Cd\mathbf{L1}H]^{2+}$ (Figure S2, Supporting Information) can be seen. Consequently, even if the Cd(II) coordination sphere is maintained in solution, the data indicated that at least two configurations can exist in solution as for similar cyclam complexes.[21,22]

For the Zn(II) complex and in absence of monocrystals, the molecular structure was investigated by NMR spectroscopy. The ^{13}C NMR spectrum of the $[Zn\mathbf{L1}H]^{2+}$ complex, for which the formula was determined by elemental analysis and mass spectroscopy, displays seven resonances for the aromatic carbons (see Experimental Section). As previously mentioned for the corresponding Cd(II) complex, the aromatic carbon region, more resolved for the zinc complex than for the free ligand, is the hallmark of the benzimidazole coordination to the metal ion.[19] Consequently, the hypothesis that $[Zn\mathbf{L1}H]^{2+}$ has a molecular structure closely related to the one of $[Cu\mathbf{L1}H]^{2+}$ can be formulated. Finally, the analysis

Table 1. Equilibrium Constants for the Protonation (log K_{01h}) and the Metal Complexation (log K_{11h}) of L1H Potentiometrically Determined at 298.1(1) K, I = 1 (KNO_3)[a]

	log $K_{01\,h}$	
reaction	**L1**H	**L2**H[10a]
$\mathbf{L}^b + H^+ = \mathbf{L}H$	12.0 (3)	11.05
$\mathbf{L}H + H^+ = \mathbf{L}H_2^+$	11.5 (2)	10.21
$\mathbf{L}H_2^+ + H^+ = \mathbf{L}H_3^{2+}$	9.73 (7)	9.01
$\mathbf{L}H_3^{2+} + H^+ = \mathbf{L}H_4^{3+}$	3.93 (9)	4.55
$\mathbf{L}H_4^{3+} + H^+ = \mathbf{L}H_5^{4+}$	2.62 (6)	<2
$\mathbf{L}H_5^{4+} + H^+ = \mathbf{L}H_6^{5+}$	1.4 (2)	<2

	log $K_{11\,h}$		
reaction	Cu(II)	Zn(II)	Cd(II)
$M + \mathbf{L}H = M\mathbf{L}H$	23.4 (1)	17.45 (5)	14.35 (3)
$M\mathbf{L}H = M\mathbf{L}^- + H^+$	−10.2 (1)	−8.49 (4)	−9.55 (2)

[a] Values in parentheses are the standard deviation on the last significant figure. [b] For **L**H ligands, the **L** species corresponds to the anionic form of the ligand.

of the ^1H aromatic ring methylene linker signals indicate that these two diastereotopic protons appear as a doublet of doublet (Figure S3, Supporting Information). For $[Zn\mathbf{L1}H]^{2+}$, the ^1H NMR spectrum reveals therefore the presence of only one stereoisomer in solution.

Potentiometric Studies. Besides these structural informations, it is interesting to give a comparative insight of the thermodynamic stability of $[Cu(\mathbf{L1}H)]^{2+}$, $[Zn(\mathbf{L1}H)]^{2+}$, and $[Cd(\mathbf{L1}H)]^{2+}$. For that, the determination of their overall stability constants by means of potentiometric measurements can be carried out. It implies first the determination of **L1**H protonation constants since protons can act as competitors for metal cations.

Table 1 summarizes the protonation constants (log $K_{01\,h}$) of **L1**H (2×10^{-3} mol dm^{-3}) potentiometrically determined in 10^{-2} mol dm^{-3} HNO_3 with I = 1 (KNO_3) at 298.1 K. Six protonation constants were calculated by using the PROTAF software.[23] Since the number of constants shown by the ligand is superior to the number of secondary and tertiary macrocyclic amine functions, it significates that the benzimidazole moiety is involved in the protonation sequence. By comparison with the protonation constants of the macrocyclic nitrogen atoms in 1,4,8,11-tetraazacyclotetradecane (cyclam, log K = 11.58, 10.62, 1.61, 2.42)[24] and 1-(pyridin-2-ylmethyl)-1,4,8,11-tetraazacyclotetradecane (cyclam-pyridine, log K = 11.31, 10.47, 2.32, 1.73),[13b] the four **L1**H protonation constants 11.5 (log K_{012}), 9.73 (log K_{013}), 2.62 (log K_{015}), 1.4 (log K_{016}) can be associated, to the acid−base equilibria on the macrocyclic nitrogen atoms. Thus for **L1**H, the remaining log K_{011} and log K_{014} values (12.0 and 3.93, respectively) could be ascribed to the benzimidazole moiety. These two latter acid−base steps can be investigated more precisely in the whole pH range, by following the pH-dependent chemical shift of the Hα and Hβ benzimidazole protons (Figure 2). A prior study on the cyclen analogue **L2**H (1-(benzimidazol-2-ylmethyl)-1,4,7,10-tetraazacyclododecane, Scheme 1) has indeed shown that the aromatic protons of the benzimidazole ring are very sensitive to the protonation degree of the aromatic ring.[10a] At pH 1.6, the benzimidazole protons appear as an AA′BB′ system. For these protons, the presence of two signals is indicative of a local C2 symmetry for the aromatic ring and then of a rapid proton exchange between the

dx.doi.org/10.1021/ic102521g |*Inorg. Chem.* 2011, 50, 4029–4038

Scheme 2

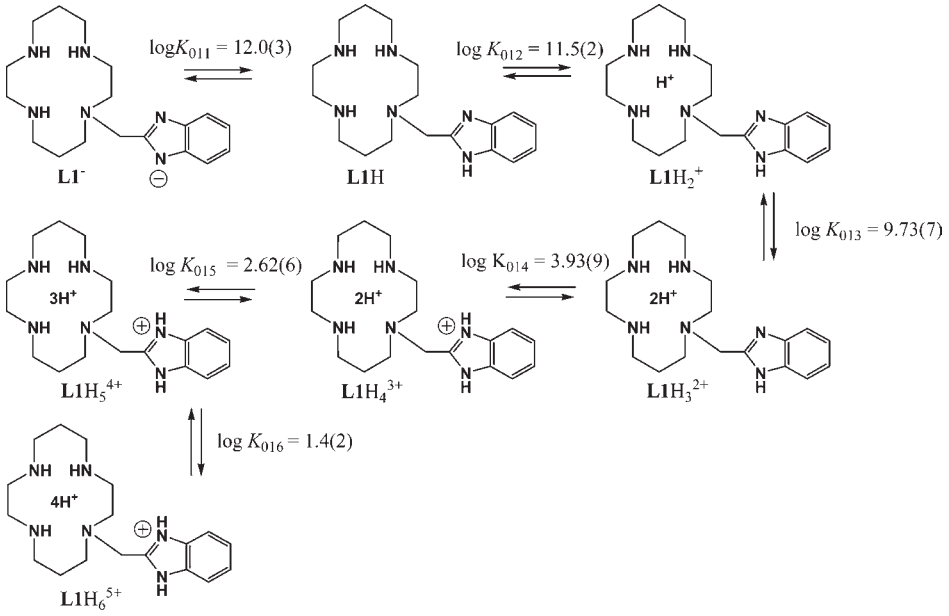

two nitrogen atoms of the benzimidazole.[25] From pH 3 to pH 5, the two signals were undergoing an upfield shift (0.30 ppm for Hβ and 0.15 ppm for Hα), leading to a spectrum which was not significantly evolving until pH 11. From this value, a second upfield shift was then observed, especially for Hβ. These consecutive variations could be considered as the result of the electronic density increase on the aromatic ring. Thus, below pH 5 (log K_{014}), the acid−base equilibrium could be associated to the protonation of the benzimidazole ring while above pH 11 (log K_{011}) the deprotonation of the benzimidazole pyrrole function should occur. Consequently in the whole pH range, the acid−base behavior of **L1**H can be summarized as in Scheme 2.

The **L1**H affinity toward Cu(II), Zn(II), and Cd(II) was then determined potentiometrically (Table 1). With each metal ion, two species are formed in solution. The first one corresponds to the $[M\mathbf{L1}H]^{2+}$ complexes. The stability of these complexes follows the ascending order Cd**L1**H < Zn**L1**H < Cu**L1**H, that is, the known Irving−Williams order for the first row transition metal ions. Another way to compare the affinity of **L1**H toward these cations is to determine the amount of free metal relative to the metal coordinated to the ligand on the whole pH range (Figure S4, Supporting Information). One can notice that above pH 5, this amount is 3 orders of magnitude higher for Zn(II) in comparison with Cu(II), and for Cd(II), this value is at least 1 order of magnitude higher than for Zn(II). In addition, the comparison of **L1**H and cyclam affinities for the three metal ions (Table S3, Supporting Information) shows that **L1**H has an affinity at least similar or even better than cyclam. This can be correlated to the additional stabilizing interaction between the benzimidazole ring and the metal which counterbalanced the weakening of the macrocyclic ligand field due the poorer σ-donor ability of tertiary amines relative to that of secondary ones.[26] The potentiometric measurements also indicate that each complex formation is followed by its deprotonation ($[M\mathbf{L1}]^+$ species). This deprotonation can be confirmed for $[Zn\mathbf{L1}H]^{2+}$ and $[Cd\mathbf{L1}H]^{2+}$ by the evolution of the ^{1}H NMR chemical shifts of Hα and Hβ aromatic protons for pH greater than 7 (Figure 4). Thus, around pH 8.5 for $[Zn\mathbf{L1}H]^{2+}$ and pH 9.5 for $[Cd\mathbf{L1}H]^{2+}$, the ^{1}H signals for Hα, and Hβ are shifted upfield ($\Delta(\delta, [Zn\mathbf{L1}H]^{2+})$ = 0.15 ppm for Hα, 0.25 ppm for Hβ; $\Delta(\delta, [Cd\mathbf{L1}H]^{2+})$ = 0.15 ppm for Hα, 0.25 ppm for Hβ). This shielding indicates a decrease in the overall charge of the complex which corresponds to the ionization of the pyrrole hydrogen of the benzimidazole moiety.[10a] Moreover for $[Zn\mathbf{L1}H]^{2+}$, on increasing the pH up to 12, the UV bands of the benzimidazole unit are perturbed and undergo a slight red shift of about 5 nm (Figure S5, Supporting Information) characteristic of deprotonation of the imidazole ring.[10a]

For $[Cu\mathbf{L1}H]^{2+}$ the same phenomenon can be proved by the evolution of the λ_{max} of the copper absorption as a function of the pH (Figure 5). A bathochromic shift, which follows the deprotonation pathway of $[Cu\mathbf{L1}H]^{2+}$ is observed, with an inflection point at approximately pH 10. Thus, the deprotonation constants determined for $[Cu\mathbf{L1}H]^{2+}$, $[Zn\mathbf{L1}H]^{2+}$, and $[Cd\mathbf{L1}H]^{2+}$ (10.2, 8.49, and 9.55, respectively Table 1) are remarkably lower than that for the analogous equilibrium for **L1**H which means that the presence of metal ions and their respective Lewis acidities make the benzimidazole pyrrole hydrogen more acidic. This point is interesting since the sensing properties of benzimidazole appended ligands are greatly influenced by the deprotonation of the benzimidazole amine group.[10a]

Spectrofluorimetric Study of L1H and Cation Sensing. The fluorescent response of **L1**H (5×10^{-7} mol dm^{-3}, I = 0.1 $NaNO_3$) was first investigated in the pH range 6−12 at 298.1 K (excitation at 270 nm) (Figure 6). As the pH is raised, emission at 304 nm increases following the formation of all the species in solution from the non emissive protonated ones to the deprotonated emissive ones, that is, at pH > 8, **L1**H$_2^+$, **L1**H, and **L1**$^-$. This behavior can be rationalized in terms of variation in the intramolecular electron transfer between the electron donor (cyclam) and the acceptor (benzimidazole) orbitals. When this transfer is optimum, that is, when both parts of the ligand, cyclam, and benzimidazole are in close proximity and in a suitable orientation, the fluorescence is quenched (PET effect). For 6 < pH < 8, **L1**H$_3^{2+}$ prevails in solution (Scheme 2), and the cyclam cavity is diprotonated while the

dx.doi.org/10.1021/ic102521g |*Inorg. Chem.* 2011, 50, 4029–4038

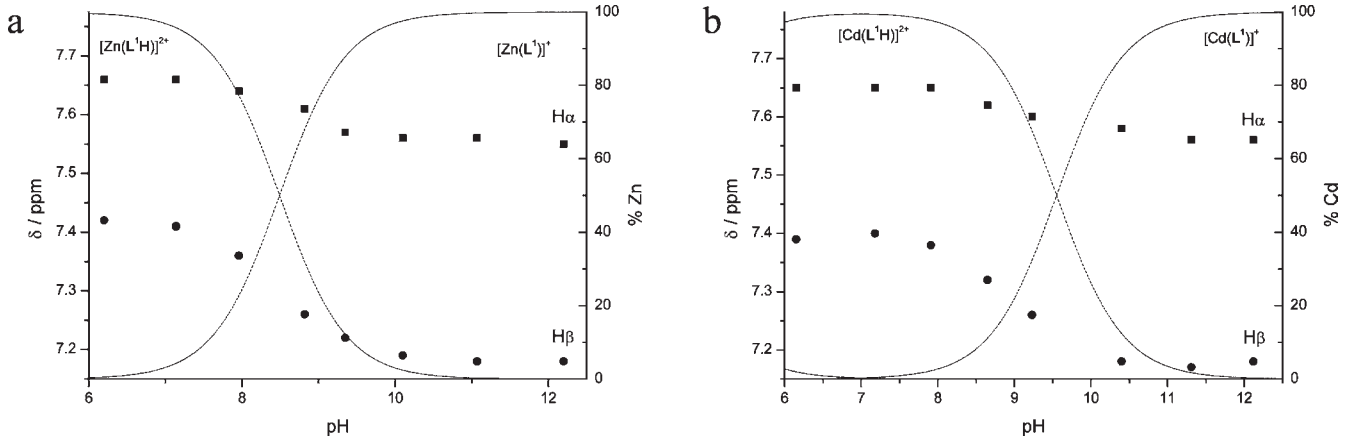

Figure 4. ^{1}H NMR chemical shifts of aromatic protons plotted as a function of pH for (a) [Zn**L1**H]$^{2+}$ and (b) [Cd**L1**H]$^{2+}$ (10^{-2} mol dm^{-3}) in the pH range 6.0−12.0 (T = 298.1 K, D_2O).

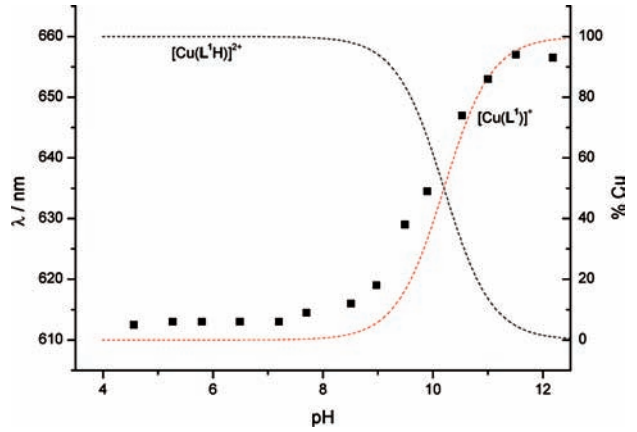

Figure 5. λ_{max} (d-d* Cu(II)) for [Cu**L1**H]$^{2+}$ as a function of pH.

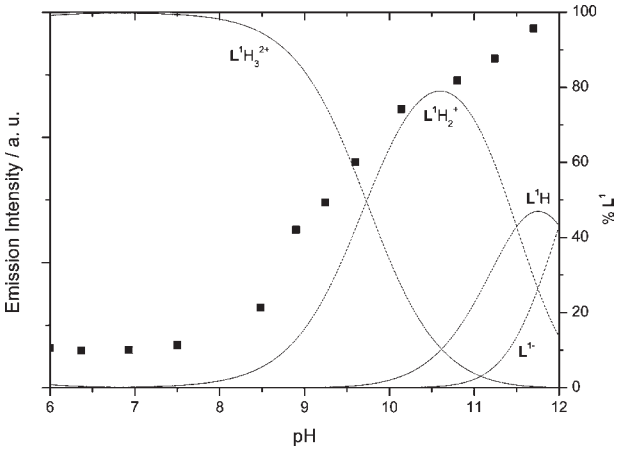

Figure 6. **L1**H fluorescence as a function of pH (5×10^{-7} mol dm^{-3}) at T = 298.1 K, excitation at 270 nm, emission at 304 nm.

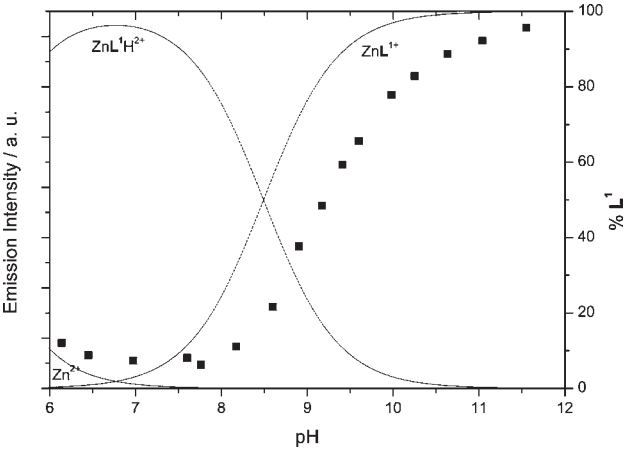

Figure 7. Zn**L1**H fluorescence as a function of pH (5×10^{-7} mol dm^{-3}) at T = 298.1 K, excitation at 270 nm, emission at 304 nm.

benzimidazole moiety is non protonated. It is known that protonated forms of macrocycles are stabilized by intramolecular hydrogen bonds between the cavity and the pendant arm (when this latter has coordinating atoms).[27] Then, the overlap between benzimidazole and cyclam is optimum, the PET effect is favored, and the species is poorly emissive. It is also known that deprotonation triggers conformational modifications that lead to outward orientation of the pendant arm relative to the macrocyclic cavity.[10a] If we assume that above pH 8 in the deprotonation sequence toward **L1**H and **L1**$^-$ similar modifications occur, then it can be expected that it results in a weak overlap between the benzimidazole and the cyclam orbitals. Consequently, the emissive deactivation of benzimidazole is favored over the PET process, and the fluorescence is restored.

In the presence of Zn(II), the evolution of the **L1**H fluorescence emission as a function of pH is presented in Figure 7. The fluorescence curve follows the formation of Zn**L1**$^+$ which means that the fluorescence intensity increased with the benzimidazole deprotonation (for pH ≥10.4, the quantum yield Φ is constant and equal to 0.19).

Upon addition of increasing quantities of Zn(II) (Figure 8), the fluorescence response of **L1**H is linear up to the addition of 1 equiv of metal as expected for the formation of a 1:1 [**L**H]/[Zn(II)] complex (see potentiometric results). This behavior is typical of a CHEF effect in which, the metal coordination makes the coordinated cyclam subunit a less efficient donor toward the benzimidazole moiety than the uncoordinated macrocycle. Consequently, the PET-type fluorescence quenching is less probable, and the native fluorescence of the

dx.doi.org/10.1021/ic102521g |*Inorg. Chem.* 2011, 50, 4029–4038

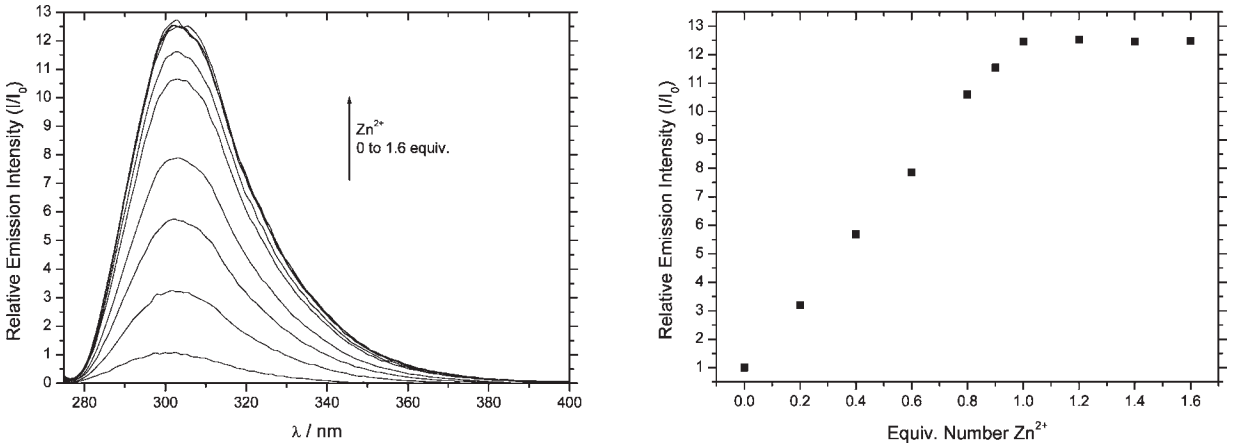

Figure 8. Change in the fluorescent response of **L1**H (5×10^{-7} mol dm^{-3}) upon addition of Zn^{2+} at pH 10.4 [CAPS (2×10^{-2} mol dm^{-3}), $I = 0.1$ (NaCl), $T = 298.1$ K, excitation at 270 nm].

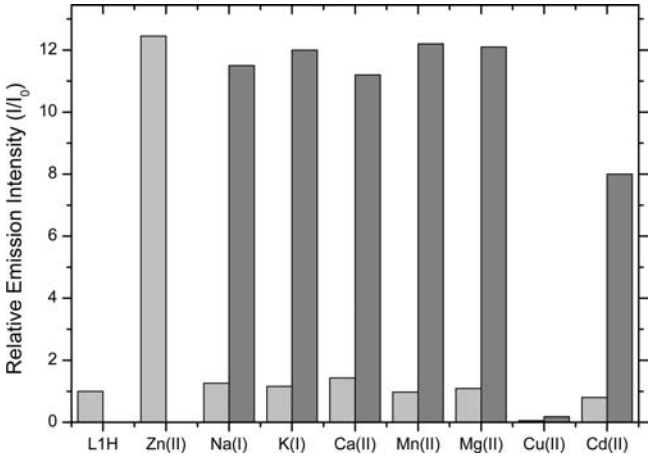

Figure 9. Relative fluorescence of **L1**H at 304 nm responding to 1 equiv of the metal ions (gray bars) and competitive binding experiments (dark gray bars) of **L1**H in which the competing metals (1.5×10^{-6} mol dm^{-3}) were added to **L1**H (5×10^{-7} mol dm^{-3}) followed by Zn(II) (5×10^{-7} mol dm^{-3}) at pH 10.4 [CAPS (2×10^{-2} mol dm^{-3}), $I = 0.1$ (NaCl), no hydroxide precipitation was observed, $T = 298.1$ K, excitation at 270 nm]. I_0 is the emission intensity of **L1**H (5×10^{-7} mol dm^{-3}) at 304 nm in the absence of metal ions.

fluorophore is thus restored.[28] The complexation gives rise to a 12-fold enhancement of the fluorescence signal with respect to the free **L1**H, with increasing [Zn(II)] (quantum yield Φ 0.02 → 0.20). In these conditions, the detection limit can be estimated at 4.5×10^{-9} mol dm^{-3} and the quantification limit at 1.5×10^{-8} mol dm^{-3}. By comparison with (benzimidazolylmethyl) cyclen **L2**H,[10a] in similar conditions **L1**H is four times more efficient to sense zinc. This efficiency which can be compared to what was described by Watkinson et al.[11] with click-generated cyclam sensors. It tends to indicate that with cyclam ligands the CHEF effect is more efficient, which induces that fluorescent cyclam ligands can be good sensor agents, even better than cyclen ones.

An important feature of any potential Zn(II) sensor is its ability to detect Zn(II) selectively over other endogenous relevant cations. The **L1**H fluorescent spectra were recorded in the presence of various metal ions at pH 10.4 (some first row transition metals, Cd(II), and biologically relevant alkali and alkaline earth ions, gray bars Figure 9). The fluorescence intensities only slightly increase by addition of ions that are found in high concentration in cells (K^+, Mg^{2+}, and Ca^{2+}). This indicates that these ions do not perturb the sensor response, which is inherent to the poor binding properties of macrocyclic polyamines toward alkali or alkaline earth cations. In the case of Cd(II), a very small difference is detected between the free ligand and the metal complex. Since the zinc complex exhibits the maximal fluorescence response, the test indicates that **L1**H allows Zn(II) and Cd(II) to be distinguished. Finally, no fluorescence is detected in the presence of Cu(II) due either to the paramagnetic-metal effect that promotes the intersystem crossing (ISC) from the S_1 state to T_1[29a] and probably to an electron donation between the fluorophore and the Cu(II).[29b]

Another important feature in a sensor is its ability to function in competition with other relevant metals (dark gray bars, Figure 9). Thus, 3-fold molar excesses of a number of metal ions were added to a solution of **L1**H prior to the addition of 1equiv of Zn(II), and their emission spectra were recorded. The addition of Zn(II) resulted in an increase of the fluorescence response of the solution, except for the Cu(II). Toward alkali or alkaline earth cations, this is in agreement with the complexation properties of cyclam ligands, that is, weak affinity for these cations, and the Zn(II) is reasonably well detected. Toward Cd(II) and Cu(II) the sensor response is governed by the relative stabilities of the complexes (Figure 3). With Cd(II), the initially formed complex Cd**L1**H is less stable than the Zn(II) one, which leads to the displacement of the equilibrium in favor of Zn**L1**H (relative to Cd**L1**H) and then to an acceptable detection of Zn(II). With Cu(II), the initially formed Cu**L1**H complex is too stable to be displaced by Zn(II), which results in quenching of the emission.

CONCLUDING REMARKS

This paper describes the coordination behavior toward Cu(II), Zn(II), and Cd(II) of a new fluorescent cyclam sensor **L1**H. The photochemical properties of this hydrosoluble ligand are PET regulated, as the ligand is non fluorescent in acidic media and emissive above pH 8. **L1**H forms stable complexes with all three metals. The fluorescence of the ligand is totally quenched by the presence of Cu(II). **L1**H behaves as an efficient OFF-ON sensor for Zn(II), even in the presence of interfering species such as alkali or alkaline earth cations because of the intrinsic

selectivity of cyclam toward transition metal ions and a high specific fluorescence response to Zn(II) due to an effective CHEF effect. The latter is much more efficient than in the cyclen analogue in similar conditions because cyclam nitrogen lone pairs are more engaged in the complexation, preventing the PET process even better. Since the development of fluorescent sensors requires an important increase in their emission upon guest interaction, fluorescent cyclams represent an efficient alternative to fluorescent cyclens because of an enhanced and selective response to biologically relevant metal ions like Zn(II).

EXPERIMENTAL SECTION

General Information. All solvents were HPLC grade. The metals salts were purchased from Aldrich. The other reagents used were of the highest commercial quality without further purification.

Ligand Synthesis. **L1**H was synthesized according to a published procedure[12] by alkylation of cyclam glyoxal ligand with 2-(chloromethyl) benzimidazole (1.51 g, 6.8 mmol) in tetrahydrofuran (THF, 10 mL) in the presence of 1 equiv of sodium iodide (1.02 g, 6.8 mmol). The solution was stirred for 2 days until a pale yellow solid precipitates. This solid which corresponds to an alkylated bis-aminal monosalt was separated from the mother solution by filtration and allowed to be deprotected with hydrazine monohydrate for 9 h at 100 °C. After cooling, a yellow solid precipitated and was collected by filtration. After several solubilization in EtOH-evaporation cycles, **L1**H was finally obtained in 86% yield (1.93 g).

^{1}H NMR (250 MHz, D_2O, 298.1 K, pH = 6.6): δ = 1.84 (2H, br s, CH_2CH_2N), 2.04 (2H, br s, CH_2CH_2N), 2.9−3.3 (16H, m, CH_2CH_2N), 3.98 (2H, br, NCH_2Car), 7.32 (2H, m, Hβ), 7.66 (2H, m, Hα). ^{13}C NMR (62.9 MHz, DMSO-d^6, 298.1 K): δ = 28.0, 30.0 (CH_2CH_2N), 49.0, 49.2, 50.0, 50.1, 50.2, 51.0, 53.2, 55.6, 57.0 (CH_2N), 116.8, 123.3, 140.9, 156.0 (Car). ESI-MS: m/z 331.4 (M+H$^+$). Calcd for $\{[C_{18}H_{30}N_6]\text{-}H\}^+$: 331.3. Anal. For $C_{18}H_{30}N_6$ (330.47 g·mol^{-1}) Calcd (Found): C, 65.42 (65.15); H, 9.15 (9.09); N, 25.43 (25.10). UV−vis: (H_2O, pH = 10.4): λ_{max} (nm) = 272; ε (M^{-1} cm^{-1}) 8000.

Synthesis of [ZnL1H](NO$_3$)$_2$ and [CdL1H(NO$_3$)](NO$_3$). To obtain [Zn**L1**H](NO$_3$)$_2$ or [Cd**L1**H(NO$_3$)](NO$_3$), a methanolic solution of the corresponding nitrate salt (0.5 mmol, 5 mL) was added dropwise to a solution of **L1**H (165 mg, 0.5 mmol) in methanol (10 mL). The colorless solution was refluxed for 5 h and concentrated by evaporation. A white powder was precipitated by addition of diethyl ether (85% yield for the Zn(II) complex, m = 229 mg, 80% yield for the Cd(II) complex, m = 237 mg).

[ZnL1H](NO$_3$)$_2$. ^{1}H NMR (250 MHz, D_2O, 298.1 K, pH = 4.32): δ = 1.6−2.2 (4H, m, CH_2CH_2N), 2.5−3.5 (16H, m, CH_2CH_2N), 3.98 (1H, d, J = 17.5 Hz, NCH_2Car), 4.44 (1H, d, J = 17.5 Hz, NCH_2Car), 7.44 (2H, m, Hβ), 7.67 (2H, m, Hα). ^{13}C NMR (62.9 MHz; DMSO-d^6, 298.1 K): δ = 23.9, 26.6 (CH_2CH_2N), 44.3, 45.5, 47.0, 47.9, 48.8, 50.3, 50.8, 53.4, 55.2 (CH_2N), 112.0, 116.6, 122.9, 123.7, 133.4, 137.6, 154.2 (Car). ESI-MS: m/z 456.2. Calcd for $[Zn(C_{18}H_{30}N_6)(NO_3)]^+$ 456.2. m/z 393.1. Calcd for $[Zn(C_{18}H_{29}N_6)]^+$ 393.2. Anal. For $C_{18}H_{30}N_8ZnO_6$. H_2O (537.91 g·mol^{-1}) Calcd (Found): C, 40.19 (40.33); H, 6.00 (5.69); N, 20.83 (20.50). UV−vis (H_2O, pH = 10.4): λ_{max} (nm) = 276; ε (M^{-1} cm^{-1}) = 7600.

[CdL1H(NO$_3$)](NO$_3$). ^{1}H NMR (250 MHz, D_2O, 298.1 K, pH = 7.18): δ = 1.6−2.0 (4H, m, CH_2CH_2N), 2.5−3.4 (16H, m, CH_2CH_2N), 3.94−4.35 (2H, m, NCH_2Car), 7.39 (2H, m Hβ), 7.63 (1H, m, Hα), 7.68 (1H, m, Hα). ^{13}C NMR (62.9 MHz; DMSO-d^6, 298.1 K): δ = 24.9, 26.2 (CH_2CH_2N), 44.4, 45.9, 49.1, 49.8, 49.9, 50.1, 53.5, 55.3, 59.8 (CH_2N), 113.1, 117.6, 123.8, 124.3, 134.0, 139.5, 155.2 (Car). ESI-MS: m/z: 506.2. Calcd for $[Cd(C_{18}H_{30}N_6)(NO_3)]^+$ 506.1. m/z 443.2. Calcd for $[Cd(C_{18}H_{29}N_6)]^+$ 443.1 Anal. For $C_{18}H_{30}N_8CdO_6$. $1.5H_2O$ (593.91 g·mol^{-1}) Calcd (Found): C, 36.40(36.55); H, 5.60(5.29); N, 18.87(18.60). UV−vis (H_2O, pH = 10.4): λ_{max} (nm) = 277; ε (M^{-1} cm^{-1}) = 8000.

Synthesis of [CuL1H](BF$_4$)$_2$. 0.2 mmol of $Cu(BF_4)_2$, $6H_2O$ (69 mg) were dissolved in 5 mL of methanol and were subsequently added dropwise to 5 mL of methanol containing 0.2 mmol of **L1**H (67 mg). The resulting blue solution was refluxed for 2 h before being concentrated; addition of diethyl ether to this solution caused the precipitation of the complex (0.09 g, 78%).

ESI-MS: m/z: 480.2. Calcd for $[Cu(C_{18}H_{30}N_6)(BF_4)_2]^+$ 480.2. m/z: 392.2. Calcd for $[Cu(C_{18}H_{29}N_6)]^+$ 392.2. Anal. For $C_{18}H_{30}N_6CuB_2F_8$. $0.5H_2O$ (576.63 g·mol^{-1}) Calcd (Found): C, 37.49 (37.68); H, 5.38(5.31); N, 14.57(14.27). UV−vis (H_2O, pH = 10.4):λ_{max} (nm) = 278; ε(M^{-1} cm^{-1}) 10300, λ_{max} (nm) = 618; ε (M^{-1} cm^{-1}) 110.

Potentiometric Measurements. Potentiometric titrations were carried out with an automatic titrator composed of a microprocessor buret Metrohm dosimat 665 and a pH meter Metrohm 713 connected to a computer. The titration procedure was fully automated.[23] All measurements were performed within a thermoregulated cell at 298.1 ± 0.1 K under an argon stream to avoid the dissolution of carbon dioxide. The ionic strength was adjusted to 1 with potassium nitrate. The combined Type "U" glass electrode Metrohm used had a very low alkaline error. The complex formation constants were determined according to the "batch method". Equimolar mixtures of Zn(II) and ligand (2×10^{-3} mol dm^{-3} in HNO_3 10^{-2} mol dm^{-3}, I = 1(KNO_3)) were prepared in 30 stoppered flasks at different pH (pH < 8) values by microaddition of KOH (10^{-1} mol dm^{-3}, I = 1(KNO_3)). These solutions were stored under argon 4 and 6 weeks, respectively, at 40 °C. Before pH measurements, these solutions were finally allowed to reach equilibrium temperature (298.1 K) for 48 h. The deprotonation of the zinc-benzimidazole complex was determined by a pH-titration of a complex solution (2×10^{-3} mol dm^{-3}, I = 1(KNO_3)) prepared from the solid [Zn**L1**H](NO_3)$_2$, monohydrate complex previously described. The protometric data were processed by using the PROTAF program[23] to obtain the best fit chemical model and refined overall constants β_{mlh}.

$$mM + lL + hH^+ \rightleftharpoons M_mL_lH_h \qquad \beta_{mlh} = \frac{[M_mL_lH_h]}{[M]^m[L]^l[H^+]^h}$$

a negative h value referring to the hydroxide ion (except for the proton, the charges are not shown for clarification).

The stepwise equilibrium constants (K_{mlh}) related to equilibrium (1) are defined by eq 2 and were deduced from the refined (β_{mlh}) values by relation 3:

$$MLH_{h-1} + H^+ \rightleftharpoons MLH_h \quad (1)$$

$$K_{mlh} = \frac{[MLH_h]}{[MLH][H^+]} \quad (2)$$

$$\beta_{mlh} = \prod_{i=1}^{h} K_{mli} \quad (3)$$

Spectroscopic Measurements. ^{1}H and ^{13}C NMR spectra were recorded on a Bruker DRX 500 spectrometer. ^{1}H−^{1}H and ^{1}H−^{13}C 2D correlation experiments were performed to assign the signals. In ^{1}H NMR titrations, the pD was adjusted by additions of small amounts of a 4% diluted NaOD solution or a 3.5% diluted DCl solution to D_2O solutions containing the ligand **L1**H (10^{-2} mol dm^{-3}). The pH was calculated from the measured pD values using eq 4:[30]

$$pH = pD - 0.40 \quad (4)$$

For both ligands, NMR measurements were performed after an equilibration time of 1 day.

Mass spectra in acetonitrile were recorded on a Micromass Q-TOF electrospray positive ionization. For both ligand and complex [Zn**L1**H](ClO_4)·$2H_2O$ (3×10^{-5} mol dm^{-3}), the UV spectrophotometric titrations

dx.doi.org/10.1021/ic102521g |Inorg. Chem. 2011, 50, 4029–4038

Table 2. Details for the Structure Determination of (a) $[CuL1H](BF_4)_2$ and (b) $[Cd(L1H)(NO_3)](NO_3)$

	(a) $[CuL^1H](BF_4)_2$, CH_3OH	(b) $[Cd(L^1H)(NO_3)](NO_3)$
empirical formula	$C_{19}H_{34}B_2CuF_8N_6O$	$C_{18}H_{30}N_8O_6Cd$
formula weight	599.68	566.9
temperature [K]	120(2)	100(2)
crystal system	monoclinic	tetragonal
space group	$P2_1$	$P42bc$
color	blue	colorless
a [Å]	8.282(3)	24.0508(14)
b [Å]	13.350(4)	24.0508(14)
c [Å]	11.660(4)	8.8378(5)
α [deg]	90.00	90
β [deg]	95.55(2)	90
γ [deg]	90.00	90
volume [Å^3]	1283.1(7)	5112.1(4)
Z	2	8
D_{calc} [g cm^{-3}]	1.55	1.47
absorption coefficient [mm^{-1}]	0.934	0.901
F[000]	618	2320
λ(Mo Kα), [Å]	0.71069	0.71073
no. independent refl	4197	5827
abs struc parameter	0.03(4)	0.007(18)
no. obs refl [$I > 2.0\ \sigma\ (I)$]	3895	5616
R_1 (obs refl)	0.0836	0.028
wR_2 (all data)	0.1943	0.0592

were recorded at 298.1 K in 200−400 nm range with a Shimadzu UV 2401 PC spectrophotometer equipped with a standard syringe shipper and a temperature-controlled TCC-240A cell holder. The experiments were monitored in the concentration range used for the pH titration; averages of 25 spectra were recorded in the pH range from 3 to 11.5. For the UV-pH titrations, the pH was adjusted by addition of small amounts of KOH (10^{-1} to 10^{-3} mol dm^{-3}) and HCl solutions (10^{-1} to 10^{-2} mol dm^{-3}). The solid state UV−vis spectra were recorded on a Varian Cary 5000 spectrophotometer completed by internal diffuse reflectance accessories.

Crystal Structure Determination. The crystal diffraction data of $[Cd(L1H)](NO_3)_2$ were collected at 120 K on a Kappa CCD diffractometer (Centre de Diffractométrie X, Univ. Rennes, France) using monochromated Mo Kα radiation (λ = 0.71073 Å). Data collection was performed with the COLLECT program.[31] Frames integration and data reduction procedures were realized using the DENZO and SCALEPACK program of the KappaCCD software package respectively[32] and with EVAL[33] and SADABS[34] programs. The structure was solved using the direct methods program SIR97,[35] that revealed all non-hydrogen atoms. SHELXL97[36] was used to refine the structure. Finally hydrogen atom were placed geometrically and held in riding mode in the least-squares refinement procedure. Final difference maps revealed no significant maxima.

For $[Cu(L1H)](BF_4)_2$, the X-ray intensity data were collected at 120 K with a MAR345 image plate using Mo Kα (λ= 0.71069 Å) radiation (Institut IMCN, Louvain la Neuve). The crystal was chosen, mounted in inert oil, and transferred to the cold gas stream for flash cooling. The best crystal with a plate-like shape was very small and very fragile. A total of 15638 reflections were collected, 4197 independent (R_{int}= 0.058), 3895 observed. The structure was solved by direct methods and refined by full-matrix least-squares on F^2 using SHELXL97.[36] All the non-hydrogen atoms, except C of the methanol molecule, were refined anisotropically. High agitation of the solvent (CH_3OH) and BF_4^- anions is observed; this explains the relatively high R indices. R values: R_1 = 0.084 for 3895 $F_o > 4\sigma(F_o)$ and 0.088 for all 4197 data; wR_2 = 0.198, S = 0.352. Flack x parameter = 0.03(4).

Crystallographic data and refinement parameters are reported in Table 2.

CCDC 800652 for $[Cd(L1H)](NO_3)_2$ and 800653 for $[Cu(L1H)](BF_4)_2$ contain the supplementary crystallographic data for this paper. These data can be obtained free of charge from Cambridge Crystallographic Data Centre via www.ccdc.cam.ac.uk/data_request/cif.

Spectrofluorimetric Measurements. Fluorescence emission spectra were recorded at 298.1 K on a Perkin-Elmer LS50B spectrofluorimeter equipped with a Hamamatsu R928 photomultiplier. The linearity of the fluorescence emission versus the concentration was checked in the concentration range 0 to 10^{-6} mol dm^{-3}. Emission spectra were normalized by the manufacturer-supplied correction curves. Quantum yields were determined by comparison of the integrated corrected emission spectrum of standard quinine sulfate[37] (the quantum yield (Φ) is 0.55). Spectrofluorimetric pH titrations of the ligand and the complex were performed as follows: the stock solutions of the ligand or the complex (ca. 3×10^{-5} mol dm^{-3}) were prepared by dissolving an appropriate amount of the ligand in a 50 mL volumetric flask and diluting with degassed water under argon atmosphere. The solution [L1H] = 5×10^{-7} mol dm^{-3} was prepared by appropriate dilution of the stock solution. The response of the ligand L1H according to increased amounts of Zn^{2+} was checked as follows: successive volumes of $Zn(ClO_4)_2 \cdot 6H_2O$ (1.2×10^{-3} mol dm^{-3}) were added to ligand solutions (3×10^{-5} mol dm^{-3}) for a constant pH value (CAPS buffer solution (2×10^{-2} mol dm^{-3}). These solutions were further diluted in CAPS buffer to reach a L1H concentration of 5×10^{-7} mol dm^{-3}. The emission spectra of ligand and complex solutions were recorded after excitation at a wavelength of λ = 270 nm in the range 275−400 nm (slit width of 5 nm).

■ ASSOCIATED CONTENT

Supporting Information. Table of selected bond distances and angles for $[CuL^1H]^{2+}$ and $[Cd(L^1H)(NO_3)]^+$,

EPR parameters for $[Cu(\mathbf{L^1}H)]^{2+}$, stability constants for the M(II)/$\mathbf{L^1}$H systems, visible spectra of $[Cu(\mathbf{L^1}H)](BF_4)_2$ in solid state and solution, ^{1}H NMR of $[Cd\mathbf{L^1}H(NO_3)]^+$ aromatic and N−CH_2 methylene linker protons, ^{1}H NMR of $[Zn\mathbf{L^1}H]^{2+}$ N−CH_2 methylene linker protons in D_2O, $[M]_{free}/[M]_{total}$ for each [M**L1**H] system, UV spectra of $[Zn(\mathbf{L^1}H)](BF_4)_2$ between pH 7 and 12, crystallographic data in CIF format. This material is available free of charge via the Internet at http://pubs.acs.org.

AUTHOR INFORMATION

Corresponding Author

*Phone: +33 326913330. Fax: +33 326913243. E-mail: françoise.chuburu@univ-reims.fr.

ACKNOWLEDGMENT

We thank D. Harakat (Université de Reims Champagne Ardenne, France) for its help with ESI-MS measurements. T. Roisnel is gratefully acknowledged for the crystal structure determination of $[Cd(\mathbf{L1}H)](NO_3)_2$.

REFERENCES

(1) (a) Drewry, J. A.; Gunning, P. T. *Coord. Chem. Rev.* **2011**, *255*, 459. (b) Domaille, D. W.; Que, E. L.; Chang, C. J. *Nat. Chem. Biol.* **2008**, *4*, 168. (c) Basabe-Desmonts, L.; Reinhoudt, D. N.; Crego-Calama, M. *Chem. Soc. Rev.* **2007**, *36*, 993.

(2) (a) Kimura, E.; Koike, T. *Chem. Soc. Rev.* **1998**, *27*, 179. (b) Jiang, P.; Guo, Z. *Coord. Chem. Rev.* **2004**, *248*, 205. (c) Maret, W.; Li, Y. *Chem. Rev.* **2009**, *109*, 4682.

(3) Cox, E. H.; Mc Lendon, G. L. *Curr. Opin. Chem. Biol.* **2000**, *4*, 162.

(4) (a) Coleman, J. E. *Curr. Opin. Chem. Biol.* **1998**, *2*, 222. (b) Lippard, S. J.; Berg, J. M. *Principles of Bioionorganic Chemistry*; De Boeck University: Brussels, Belgium, 1997.

(5) Burdette, S.; Lippard, S. J. *Coord. Chem. Rev.* **2001**, *216−217*, 333.

(6) (a) Prodi, L. *New. J. Chem.* **2005**, *29*, 20. (b) Czarnik, A. W. *Fluorescent Chemosensors for Ion and Molecule Recognition*; American Chemical Society: Washington, DC, 1993.

(7) (a) de Silva, A. P.; Gunaratne, H. Q. N.; Gunnlaugsson, T.; Huxley, A. J. M.; McCoy, C. P.; Rademacher, J. T.; Rice, T. E. *Chem. Rev.* **1997**, *97*, 1515. (b) Valeur, B.; Leray, I. *Coord. Chem. Rev.* **2000**, *205*, 3. (c) Prodi, L.; Bolletta, F.; Montaldi, M.; Zaccheroni, N. *Coord. Chem. Rev.* **2000**, *205*, 59.

(8) Nolan, E. M.; Lippard, S. J. *Acc. Chem. Res.* **2009**, *42*, 193, and references therein.

(9) (a) Kimura, E.; Aoki, S.; Kikuta, E.; Koike, T. *Proc. Natl. Acad. Sci. U.S.A.* **2003**, *100*, 3731. (b) Carol, P.; Sreejith, S.; Ajayaghosh, A. *Chem. Asian J.* **2007**, *2*, 338. (c) Akkaya, E. U.; Huston, M. E.; Czarnik, A. W. *J. Am. Chem. Soc.* **1990**, *112*, 3590. (d) Koike, T.; Watanabe, T.; Aoki, S.; Kimura, E.; Shiro, M. *J. Am. Chem. Soc.* **1996**, *118*, 12696. (e) Aoki, S.; Kaido, S.; Fujioka, H.; Kimura, E. *Inorg. Chem.* **2003**, *42*, 1023. (f) Aoki, S.; Sakurama, K.; Matsuo, N.; Yamada, Y.; Takasawa, R.; Tanuma, S.; Shiro, M.; Takeda, K.; Kimura, E. *Chem.—Eur. J.* **2006**, *12*, 9066. (g) Hirano, T.; Kikuchi, K.; Urano, Y.; Higuchi, T.; Nagano, T. *Angew. Chem., Int. Ed.* **2000**, *39*, 1052. (h) Burdette, S. C.; Lippard, S. J. *Inorg. Chem.* **2002**, *41*, 6816. (i) Aoki, S.; Sakurama, K.; Ohshima, R.; Matsuo, N.; Yamada, Y.; Takasawa, R.; Tanuma, S.; Takeda, K.; Kimura, E. *Inorg. Chem.* **2008**, *47*, 2747. (j) Aoki, S.; Sakurama, K.; Matsuo, N.; Yamada, Y.; Takasawa, R.; Tanuma, S.; Shiro, M.; Takeda, K.; Kimura, E. *Chem.—Eur. J.* **2006**, *12*, 9066.

(10) (a) El Majzoub, A.; Cadiou, C.; Déchamps-Olivier, I.; Chuburu, F.; Aplincourt, M. *Eur. J. Inorg. Chem.* **2007**, 5087. (b) El Majzoub, A.; Cadiou, C.; Déchamps-Olivier, I.; Chuburu, F.; Aplincourt, M.; Tinant, B. *Inorg. Chim. Acta* **2009**, *362*, 1169.

(11) (a) Tamanini, E.; Katewa, A.; Sedger, L. M.; Todd, M. H.; Watkinson, M. J. *Inorg. Chem.* **2009**, *48*, 319. (b) Tamanini, E.; Flavin, K.; Motevalli, M.; Piperno, S.; Gheber, L. A.; Todd, M. H.; Watkinson, M. *Inorg. Chem.* **2010**, *49*, 3789.

(12) Le Baccon, M.; Chuburu, F.; Toupet, L.; Handel, H.; Soibinet, M.; Déchamps-Olivier, I.; Barbier, J. P.; Aplincourt, M. *New J. Chem.* **2001**, *25*, 1168.

(13) (a) Bosnich, B.; Poon, C. K.; Tobe, M. L. *Inorg. Chem.* **1965**, *4*, 1102. (b) El Ghachtouli, S.; Cadiou, C.; Déchamps-Olivier, I.; Chuburu, F.; Aplincourt, M.; Roisnel, T. *Eur. J. Inorg. Chem.* **2006** 3472.

(14) Hathaway, B. J. *J. Chem. Soc., Dalton Trans.* **1972**, 1196.

(15) Hathaway, B. J.; Tomlinson, A. A. G. *Coord. Chem. Rev.* **1970**, *5*, 1.

(16) Miyoshi, K.; Tanaka, H.; Kimura, E.; Tsuboyama, S.; Murata, S.; Shimizu, H.; Ishizu, K. *Inorg. Chim. Acta* **1983**, *78*, 23.

(17) (a) Quiroz-Castro, E.; Bernes, S.; Barba-Behrens, N.; Tapia-Benavides, R.; Contreras, R.; Noth, H. *Polyhedron* **2000**, *19*, 1479. (b) Grevy, J.-M.; Tellez, F.; Bernes, S.; Noth, H.; Contreras, R.; Barba-Behrens, N. *Inorg. Chim. Acta* **2002**, *339*, 532.

(18) (a) Niu, W.; Wong, E. H.; Weisman, G. R.; Hill, D. C.; Tranchemontagne, D. J.; Lam, K. C.; Sommer, R. D.; Zakharov, L. N.; Rheingold, A. L. *Dalton Trans.* **2004**, 3536. (b) Salehzadeh, S.; Golbedaghi, R.; Tidmarsh, I. S.; Al-Rasbi, N. K.; Adams, H.; Ward, M. D. *Polyhedron* **2008**, *27*, 3549. (c) Fernández-Fernández, M. d. C.; Bastida, R.; Macías, A.; Valencia, L.; Pérez-Lourido, P. *Polyhedron* **2006**, *26*, 783. (d) Dong, Y.; Farquhar, S.; Gloe, K.; Lindoy, L. F.; Rumbel, B. R.; Turner, P.; Wichmann, K. *Dalton Trans.* **2003** 1558.

(19) Regueiro-Figueroa, M.; Esteban-Gómez, D.; Platas-Iglesias, C.; de Blas, A.; Rodríguez-Blas, T. *Eur. J. Inorg. Chem.* **2007**, 2198.

(20) Spectrum acquired immediately after dissolving the sample in D_2O solution. This spectrum did not change over a period of more than two weeks.

(21) Liang, X.; Parkinson, J. A.; Weishaupl, M.; Gould, R. O.; Paisey, S. J.; Park, H. S.; Hunter, T. M.; Blindauer, C. A.; Parsons, S.; Sadler, P. J. *J. Am. Chem. Soc.* **2002**, *124*, 9105.

(22) Liang, X.; Parkinson, J. A.; Parsons, S.; Weishaupl, M.; Sadler, P. J. *Inorg. Chem.* **2002**, *41*, 4539.

(23) (a) Fournaise, R.; Petitfaux, C. *Talanta* **1987**, *34*, 385. (b) Fournaise, R.; Petitfaux, C. *Analysis* **1990**, *18*, 242.

(24) Bianchi, A.; Micheloni, M.; Paoletti, P. *Coord. Chem. Rev.* **1991**, *110*, 17.

(25) Lockart, J. C.; Clegg, W.; Stuart Hill, M. N.; Rushton, D. J. *J. Chem. Soc., Dalton Trans.* **1990**, 3541.

(26) Aoki, S.; Kaido, S.; Fujioka, H.; Kimura, E. *Inorg. Chem.* **2003**, *42*, 1023.

(27) Aoki, S.; Kagata, D.; Shiro, M.; Takeda, K.; Kimura, E. *J. Am. Chem. Soc.* **2004**, *126*, 13377.

(28) Lim, N. C.; Freake, H. C.; Bruckner, C. *Chem.—Eur. J.* **2005**, *11*, 38.

(29) (a) Gilbert, A.; Baggott, J. *Essential of Molecular Photochemistry*; Blackwell: Oxford, U.K., 1991. (b) Turro, N. J. *Modern Molecular Photochemistry*; University Science Books: Mill Valley, CA, 1991. (c) Lakowicz, J. R. *Principles of Fluorescence Spectroscopy*, 3rd ed.; Springer: New York, 2006.

(30) Delgado, R.; de Silva, J. J. R. F.; Amorim, M. T. S.; Cabral, M. F.; Chaves, S.; Costa, J. *Anal. Chim. Acta* **1991**, *245*, 271.

(31) *COLLECT: KappaCCD software*; Nonius BV: Delft, The Netherlands, 1998.

(32) Otwinowski, Z.; Minor, W. *Methods in Enzymology*; Carter, C. W., Jr., Sweet, R. M., Eds.; Academic Press: New York, 1997; Vol. 276, p 307.

(33) Altomare, A.; Burla, M. C.; Camalli, M.; Cascarano, G.; Giacovazzo, C.; Guagliardi, A.; Moliterni, A. G. G.; Polidori, G.; Spagna, R. *J. Appl. Crystallogr.* **1999**, *32*, 115.

(34) Sheldrick, G. M. *SADABS*, version 2.03; Bruker AXS Inc.: Madison, WI, 2002.
(35) Duisenberg, A. J. M. Reflections on Area Detectors, Ph.D. Thesis, Utrecht University, The Netherlands, 1998.
(36) Sheldrick, G. M. *SHELX97, Program for the Refinement of Crystal Structures*; University of Göttingen: Göttingen, Germany, 1997.
(37) Tway, P. C.; Cline Love, L. J. *J. Phys. Chem.* **1982**, *86*, 5223.